THE JOURNAL OF BIOLOGICAL CHEMISTRY VOL. 290, NO. 14, pp. 8975–8986, April 3, 2015

Photodynamic Therapy-mediated Cancer Vaccination Enhances Stem-like Phenotype and Immune Escape, Which Can Be Blocked by Thrombospondin-1 Signaling through CD47 Receptor Protein*

Received for publication, November 10, 2014, and in revised form, February 17, 2015 Published, JBC Papers in Press, February 19, 2015, DOI 10.1074/jbc.M114.624965

Yuanhong Zheng[‡], Fangyuan Zou[‡], Jingjing Wang[‡], Guifang Yin[‡], Vanminh Le[‡], Zhewei Fei[§1], and Jianwen Liu[‡2]

From the [‡]Department of Molecular and Cellular Pharmacology, Biomedical Nanotechnology Center, State Key Laboratory of Bioreactor Engineering and Shanghai Key Laboratory of New Drug Design, School of Pharmacy, East China University of Science and Technology, Shanghai, 200237, China and [§]Department of General Surgery, Xinhua Hospital Chongming Branch, Shanghai Jiaotong University School of Medicine, 25 Nanmen Road, Chengqiaozhen, Chongming Shanghai, 202150, China

Background: Photodynamic therapy (PDT)-mediated vaccination has shown poor clinical outcomes in tumor treatment.
Results: Tumor cells that escaped from PDT-mediated vaccination exhibited enhanced stem-like phenotypes and undermined immunogenicity, which were prevented by interfering TSP-1/CD47/SIRP-α signal axis.
Conclusion: TSP-1/CD47/SIRP-α signal axis is associated with the malignant evolution of tumor cells upon tumor vaccination.
Significance: This study provides new evidence for improving the clinical outcome of immunotherapy.

Like most of the strategies for cancer immunotherapy, photodynamic therapy-mediated vaccination has shown poor clinical outcomes in application. The aim of this study is to offer a glimpse at the mechanisms that are responsible for the failure based on cancer immuno-editing theory and to search for a positive solution. In this study we found that tumor cells were able to adapt themselves to the immune pressure exerted by vaccination. The survived tumor cells exhibited enhanced tumorigenic and stem-like phenotypes as well as undermined immunogenicity. Viewed as a whole, immune-selected tumor cells showed more malignant characteristics and the ability of immune escape, which might contribute to the eventual relapse. Thrombospondin-1 signaling via CD47 helped prevent tumor cells from becoming stem-like and rendered them vulnerable to immune attack. These findings prove that the TSP-1/CD47/SIRP-α signal axis is important to the evolution of tumor cells in the microenvironment of immunotherapy and identify thrombospondin-1 as a key signal with therapeutic benefits in overcoming long term relapse, providing new evidence for the clinical promise of cancer vaccination.

In the past decades cancer immunotherapy has exhibited potent antitumor efficacy in preclinical experiments (1). Photodynamic therapy (PDT)[3] is reported to be an effective antitumor vaccination strategy for cancer immunotherapy (2, 3). By inducing tumor cells to undergo immunogenic apoptosis (marked with cell surface exposure of damage-associated molecular patterns (4), PDT promotes the phagocytosis of tumor cells by dendritic cells (DCs) (5) and thus elicits tumor-specific T cell-mediated immune responses (6, 7). With the emergence of new strategies like PDT, cancer immunotherapy shows a promising development prospect. However, in clinical trials, the expected positive outcomes including tumor shrinkage and improved long term survival were not observed in treated patients (8–10).

The poor clinical outcome of tumor vaccinations has urged researchers to further investigate the mechanisms that are responsible for the failure (11, 12). One of the mechanisms proposed is cancer immuno-editing theory, in which the immune system is thought to not only protect the host against tumor formation but also to be involved in shaping tumor immunogenicity (13).

CD47 is an integrin-associated receptor protein expressed at high levels on the surface of various cancer cells. There are two important counter-receptors for CD47: thrombospondin-1 (TSP-1) and signal regulatory protein-α (SIRP-α) (14). Recent studies have shown that the TSP-1/CD47/SIRP-α signal axis mediates various cellular functions, which links with their diverse cellular distribution (15–17). In general, CD47 expressed on tumor cells is thought to inhibit the phagocytosis by signaling through SIRP-α present on macrophages and dendritic cells. It is also associated with T cell activation and induction of antigen-specific CTL responses by DCs (16, 18, 19). Moreover, ligation of CD47 by TSP-1 plays a complicated and intricate role in anti-tumor effect and immune regulation (20–22). Studies of this signal axis to date have provided new insights into the cross-talk between tumor cells and the immune system.

In this study we reported that tumor cells adapted themselves to the immune pressure exerted by vaccination. During the process, tumor cells gained enhanced tumorigenic and stem-like phenotypes as well as undermined immunogenicity,

* This work was supported by Shanghai Committee of Science and Technology Grants 13140902300 and 11DZ2260600.
[1] To whom correspondence may be addressed. Tel./Fax: 86-21-64252262; E-mail: zheweifei@xinhuamed.com.cn.
[2] To whom correspondence may be addressed. Tel./Fax: 86-21-64252044; E-mail address: liujian@ecust.edu.cn.
[3] The abbreviations used are: PDT, photodynamic therapy; DC, dendritic cell; CD47, integrin-associated protein; CTL, cytotoxic T-lymphocyte; TSP-1, thrombospondin-1; SIRP-α, signal regulatory protein-α; CT, cycle threshold; MTT, 3-(4,5-dimethylthiazol-2-yl)-2, 5-diphenyl tetrazolium bromide; LLC, Lewis lung carcinoma.

thus becoming impervious to immune surveillance and elimination. Thrombospondin-1 signaling via CD47 helped prevent tumor cells from becoming stem-like and regain their sensitivity to immune attack. Our study clarifies the significance of the TSP-1/CD47/SIRP-α signal axis in cancer immunotherapy and identifies thrombospondin-1 as a key signal with therapeutic benefits in overcoming long term relapse, providing new evidence for the clinical promise of cancer vaccination.

EXPERIMENTAL PROCEDURES

Antibodies and Reagents—Antibodies against c-Myc and Sox2 were purchased from Epitomics Inc. Anti-Klf4, anti-Oct4 antibodies, and secondary antibodies conjugated with FITC and HRP were purchased from ProteinTech Group, Inc. (Atlanta, GA). β-Actin, TSP-1, and SIRP-α antibodies were purchased from Santa Cruz Biotechnology. FITC-conjugated antibodies CD8, CD47, CD44, CD34, and CD133 and phosphatidylethanolamine-conjugated antibodies IFN-γ and appropriate isotype control antibodies were all purchased from eBioscience, Inc. Anti-cleaved caspase3 antibody was obtained from Cell Signaling Technology, Inc. (Danvers, MA). Mouse and human TSP-1, mouse recombinant basic fibroblast growth factor, and epidermal growth factor were all from R&D systems Inc. (Minneapolis, MN).

Mice—6–8-Week male BALB/c nude mice and C57BL/6 mice were purchased from the Shanghai Laboratory Animal Resource Center (Shanghai, China) and maintained in a pathogen-free temperature- and humidity-controlled environment. Food and water were available *ad libitum*. Mice were euthanized to harvest tumors or to end *in vivo* experiments at the indicated time points. All animal experiments were carried out according to the guidelines for animal care of Ministry of Science and Technology of the People's Republic of China. Ethical approval was given by the Administrative Panel on Laboratory Animal Care of the Shanghai Xinhua Hospital.

Cell Culture—Lewis lung carcinoma (LLC) cells, HCT116, A549, and HeLa cells were purchased from the Cell Bank of Type Culture Collection of Chinese Academy of Sciences (Shanghai, China). Among them, HCT116, A549, and HeLa cells were cultured in RPMI1640, whereas LLC and the immune selected cell lines were cultured in DMEM. The culture media were supplemented with 10% heat-inactivated fetal bovine serum (Gibco), penicillin (100 units/ml), and streptomycin (100 units/ml) (Invitrogen). All the cells were incubated at 37 °C in a 5% CO_2 atmosphere.

PDT Treatment, Generation of Tumor-loaded DCs, and Mice Immunization—LLC cells were treated with 0.25 mM hypericin and incubated for 16 h in the dark. Cells were irradiated with a 100-watt quartz-halogen lamp at the light dose of 1.85J/cm^2. Cells were harvested 4 h post-PDT and used for co-cultured experiments. Bone marrow-derived DCs were generated from C57BL/6 mice as described previously (7). Immature DCs (imDCs) on day6 were fed with hypericin PDT-treated LLC cells at a ratio of 5:1 (imDC:LLC) for 24 h, thus forming tumor-loaded DCs. Tumor-loaded DC cells (1×10^6) in 200 μl of PBS were injected subcutaneously into the left flank of 6-week-old male C57BL/6 mice. Immunization was performed twice a week.

In Vivo Immune Selection—Six-week-old male C57BL/6 mice were purchased from the Shanghai Laboratory Animal Resource Center (Shanghai, China) and maintained in pathogen-free conditions. LLC cells (1×10^6 in 200 μl of PBS) were injected subcutaneously into the left flank of C57BL/6 mice. Subsequent tumors formed were designated as T_0. Furthermore, new mice were immunized and re-challenged with 5×10^5 T_0 cells from the previous generation mice 7 days after the second immunization (6). The escape variant tumors were designated as T_1 and were explanted into a new group of immunized mice. The resulting tumors were designated as T_2. By repeated injections with tumor cells from the last generation of immunized mice, we performed *in vivo* immune selection and harvested tumor tissue samples from T_0 to T_3.

Cytotoxic T Lymphocyte (CTL) Generation—Spleen lymphocytes were harvested from C57BL/6 mice. The spleen lymphocytes were stimulated with PDT-treated LLC-pulsed DCs on day 0 and day 7 in the presence of IL2 (25–50 IU/ml; Peprotech). The ratio of co-culture was 1:20 (DC:T). T represents the spleen lymphocytes we harvested. The suspension cells were collected and used for the subsequent experiments as CTL.

In Vitro Immune Selection—CTLs were generated as described previously (7). For immune selection, LLC cells were co-cultured with CTLs for 24 h. The cultures were pipetted, and non-adherent cells were removed and discarded. Surviving LLC cells were designated as P_1 cells and were further cultured until the next passage. The procedure was repeated until we harvested P_2 and P_3 cell lines. Normal LLC cells were designated as P_0.

Immunohistochemistry—Mice bearing tumors were euthanized at the indicated times. T_0–T_3 tumors and normal lung tissues were fixed with formalin. Paraffin-embedded sections were prepared using standard techniques and stained for stemness factors or TSP-1 expression. Immunostaining was performed as previously described (23) using antibodies against c-Myc, Klf4, Oct4, Sox2, and TSP-1. The 3,3*N*-diaminobenzidine tetrahydrochloride (DAB) peroxidase substrate kit (Beyotime Biotech, Haimen, China) was used according to the manufacturer's instructions.

Vector Construction, Transient Transfection, and Recombinant TSP-1 Treatment—CD47 short hairpin RNA (shRNA) sequence and a control shRNA were previously described by Vermeer *et al.* (24). The oligonucleotide strands were synthesized by Generay Biotech Co., Ltd (Shanghai, China). The oligonucleotide strands were diluted with double distilled H_2O and annealed into double strands followed by insertion into the pSilencer 2.1-U6 vector (Invitrogen) to form shCD47 expression constructs.

Cells were seeded into 6-well plates at a density of 2×10^5 per well and incubated overnight to allow for cell attachment. The shCD47 vector was transfected into cells with Lipofectamine^{TM} 2000 (Invitrogen) according to the manufacturer's protocol. Four hours after transfection, the cell media were removed and discarded, and complete growth media containing 2.2 nM recombinant mouse or human thrombospondin-1 was added. At 48 h post treatment, cells were harvested and used for subsequent experiments.

Flow Cytometric Analysis—For cell surface protein expression analysis, P_0–P_3 cells were trypsinized. After washing twice in cold PBS, staining for stem cell markers or CD47 was performed as described previously (25). Samples were then analyzed by FACScan (BD Bioscience) to detect cell surface CD133, CD44, CD34, and CD47. Appropriate isotype antibodies were used as controls. Data were analyzed using Flowjo software and presented as histograms.

For cell cycle analysis, a cell cycle assay kit (Vazyme Biotech, Nanjing, China) based on propidium iodide staining was used according to the manufacturer's instructions. The cell cycle distribution in G_1, S, M, and G_2 phases was determined for at least 20,000 cells with doublet discrimination. Flowjo software was used to analyze the cell-cycle position.

Western Blot—Cell lysate was extracted and used to perform Western blot as described previously (26). β-actin was used as loading control.

CTL Assay—To determine caspase-3 activation, tumor cells with different treatments were labeled with 10 μM carboxyfluorescein succinimidyl amino ester (CFSE), a fluorescent dye for detecting living cells, for 1 h. CFSE-labeled target cells were co-incubated with CTL as effector cells at a ratio of 1:10. After incubation for 24 h at 37 °C, the tumor cells were washed and stained with anti-cleaved caspase-3 antibody described previously (27). Phosphatidylethanolamine-conjugated secondary antibody alone was used as a control. Samples were then analyzed by FACScan (BD Biosciences), and data were analyzed with Flowjo software.

CTL cytotoxicity was also evaluated using the lactate dehydrogenase release assay referred to the previous report (28).

Evaluation of T Cell Activation—Cells with or without treatment were co-cultured with CTL at a T/tumor cell ratio of 1:10 for 24 h. The IFN-γ-producing CD8+ tumor-specific T cell population was evaluated as previously described (7).

RNA Isolation, Reverse Transcription, and Quantitative Real-time PCR—Total RNA of untreated or treated cells was extracted using TRIzol (Invitrogen). cDNA was synthesized using the genomic DNA removal and cDNA synthesis kit (TransGen, Beijing, China). Real-time PCR was performed using SYBR1 Premix Ex TaqTM II (Takara Bio Inc, Dalian, China) to detect the mRNA level of stemness factors. Primers were reported previously (29). All samples were normalized to GAPDH level, and -fold change was calculated using the comparative cycle threshold (CT) method ($2^{-\Delta\Delta Ct}$) (30).

Cell Proliferation Assay—Cells were plated in 96-well plates with 1×10^3 cells/well and incubated for 4 h in regular growth medium to allow for cell attachment. Samples were either transfected with shCD47 or treated with 2.2 nM TSP-1 for 24 h. After transfection or TSP-1 treatment, the cells were cultured for 1, 2, 3, 4, and 5 days. Proliferation of cancer cells was measured using the 3-(4,5-dimethylthiazol-2-yl)-2, 5-diphenyl tetrazolium bromide (MTT) assay (31).

Tumor Sphere-forming Assay—Cells were trypsinized and resuspended with serum-free DMEM/F-12. Cells were then plated at a density of 2×10^3 cells per well in 96-well super-low adherence vessels. The serum-free DMEM/F-12 was supplemented with epidermal growth factor (20 ng/ml), basic fibroblast growth factor (20 ng/ml), and 2% B27 (Gibco). Culture medium was replaced every 3 days (32). Colonies were examined under a microscope, and those larger than 75 μm in diameter were counted as a sphere-forming unit.

Tumorigenicity Assay—P_0, P_1, P_2, and P_3 cells were trypsinized and resuspended with DMEM culture medium. BALB/c nude mice were injected subcutaneously with 2×10^3 and 2×10^4 cells, respectively. Tumor formation was monitored until 18 days post injection.

Immunofluorescence—Surface immunofluorescence was performed to detect the CD47 expression of P_0 and P_3 cells, as described previously (33). Fluorescence was observed with a Nikon A1R laser scanning confocal microscope (Nikon, Tokyo, Japan).

Co-immunoprecipitation—Immature DCs were generated from C57BL/6 mouse bone marrow progenitor cells as described previously.

Tumor cells of different groups were transfected with shCD47 or treated with 2.2 nM TSP-1. At 48 h after treatment, cells were co-cultured with immune DCs at a ratio of 1:5 for 24 h. The co-culture cell lysates were then prepared and precipitated with an anti-TSP-1 or a CD47 antibody. Protein A+G-agarose (Beyotime Biotech) was used to perform co-immunoprecipitation assays according to the manufacturer's instructions. Finally, we determined the CD47 or TSP-1 protein level by Western blot.

Statistical Analysis—All experiments were repeated more than five times, and the results are presented as the mean of those independent experiments. Two-tailed Student's *t* tests were used to assess differences between the treated and control groups. Statistical analysis was performed by GraphPad prism5 software to evaluate the significance of the difference between groups, shown as $p < 0.05$ (*), $p < 0.01$ (**), $p < 0.001$ (***) (26).

RESULTS

In Vivo Immune Selection Promotes the Tumor Growth and Tumorigenicity as Well as the Expression of Cancer Stemness Factors—Previous studies have demonstrated that tumor cells subjected to photodynamic therapy can cause phenotypic maturation of homologous dendritic cells, further inducing potent tumor-specific immune response characterized by activation of CTLs and suppression of the Treg population (5, 34). As a result, tumor cells that were subsequently added to the culture system were vulnerable to cytotoxic immune cells in both co-culture experiments *in vitro* and tumor re-challenge experiments *in vivo* (6, 7). Our previous experiments also prove that hypericin-mediated PDT can act in a similar way against LLC cells both *in vitro* and in C57BL/6 mice(data not shown).[4]

In the current study we repeated the process of vaccination and tumor re-challenge, which we termed immune selection. Our results show that after three rounds of immune selection (T_3), palpable masses were seen in all of the immunized mice within 7 days, whereas the initial generation of tumors (T_0) were generated in one of seven immunized mice in the first week (Fig. 1*A*). In addition to stronger tumorigenicity, tumors that had undergone immune selection also exhibited a faster growth rate (Fig. 1*B*). It suggests that tumor cells gain resistance

[4] Y. Zheng and J. Liu, unpublished observation.

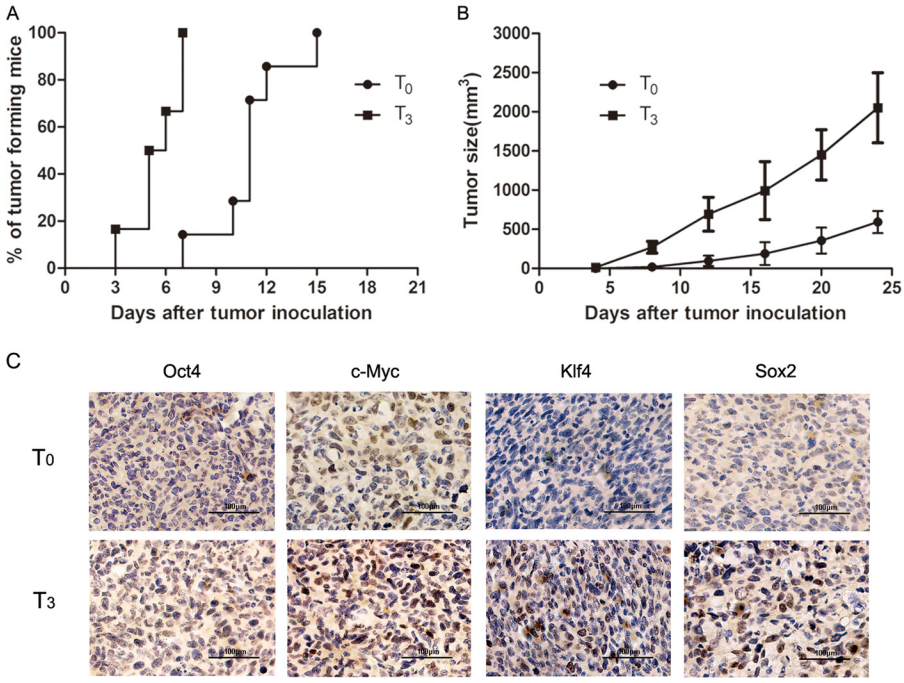

FIGURE 1. **The growth rate, tumorigenicity, and stemness factor expression of tumor cells upon *in vivo* immune selection.** *A*, tumor formation of T_0 and T_3 was monitored in the first 2 weeks post-re-challenge. Seven mice were included in each generation. The data are shown as the percentage of mice that formed tumors. *B*, tumor sizes were measured for 18 days post-re-challenge. Data are presented as the mean ± S.D. of seven mice in the T_0 and T_3 generations. *C*, representative images of immunohistochemistry for stemness factors in T_0–T_3 tumor tissues.

to the vaccine-induced tumor response during immune selection. c-Myc, Oct4, Klf4, and Sox2 are four well validated transcription factors for characterization of cancer stem cells (35, 36). Thus, they are also known as stemness factors. In Fig. 1*C*, enhanced expression of the four cancer stemness factors was observed in T_3 tumor tissue compared with T_0 tumor tissue. These changes were not observed in tumor cells that underwent normal passage *in vivo* (data not shown).

The Impact of in Vitro Immune Selection on Cell Proliferation and Stem-like Properties—We performed *in vitro* immune selection, as described previously. In *in vivo* experiments, we found that cells that had survived immune selection formed escape variant tumors with a faster growth rate and enhanced tumorigenicity. We thus evaluated the proliferative capacity, cell cycle distribution, and expression of cell cycle-associated proteins of *in vitro* immune-selected cells in each generation. The results of MTT assay showed that (Fig. 2*A*) both P_2 and P_3 cells had a faster growth rate compared with original LLC cells (P_0). The P_3 cells in particular showed a significant increase in the number of cells in the S-phase and a decrease in the number of cells in the G_0/G_1 phase (Fig. 2*B*). Correspondingly, cyclin-dependent kinase inhibitor p21 was efficiently reduced in P_2 and P_3 cells, whereas the expression of cyclin A increased (Fig. 2*C*).

Furthermore, to evaluate the change of stem-like properties of cells from P_0 to P_3, we analyzed cancer stem cell makers and sphere-forming capacity as well as the expression of stemness factors at both the protein and mRNA level. Cell surface molecules including CD44, CD133, and CD34 are frequently used for identification and isolation of cancer stem cells in lung cancer (32, 37–39). Up-regulation of these three markers was observed when immune selection was carried out to the second generation (P_2). This up-regulation was more significant in P_3 cells (Fig. 2*D*). Besides, our data showed that P_3 cells were able to generate more tumor spheres than P_0 (Fig. 2*E*). Spheres formed from P_0 and P_3 could be serially passaged to form the next spheres (data not shown). We also observed increased expression at both the mRNA and protein levels of cancer stemness factors including c-Myc, Klf4, Oct4, and Sox2 (Fig. 2, *F* and *G*). Taken together, these results indicate that immune selection *in vitro* can increase the growth rate and stem-like phenotypes.

Analysis of Immunogenicity and Tumorigenicity of Immune-selected Cells—To explore the impact of immune selection on the interaction between tumor cells and the tumor microenvironment, we first evaluated the ability of P_0-P_3 cells to activate tumor-specific T-cell responses. As shown in Fig. 3*A*, co-incubation of T cells with P_3 cells resulted in weaker activation of IFN-γ-secreting CD8+ T cells than with P_0, which suggests that vaccination selection confers tumor cells with resistance to adaptive immunity.

Besides, we evaluated CTL-mediated apoptosis by determining the frequency of cells positive for cleaved caspase-3 staining. A larger degree of apoptosis was seen in CTL-treated P_0 cells relative to CTL-treated P_3 cells (Fig. 3*B*). This result suggests that cells gradually gain a stronger capacity to escape CTL cytotoxicity upon immune selection. We also carried out CTL experiments based on lactate dehydrogenase release. As revealed in Fig. 3*C*, CTLs killed less P_3 cells ($p < 0.01$ at the effector: target ratio of 1:40) than P_0 cells.

Approximately 2×10^3–2×10^4 P_0 or P_3 cells were injected subcutaneously into the left flank of BALB/c nude mice, and tumor formation was monitored. The results in Fig. 3, *D* and *E*, show that only 1 of 7 mice challenged with 2×10^3 P_0 cells made

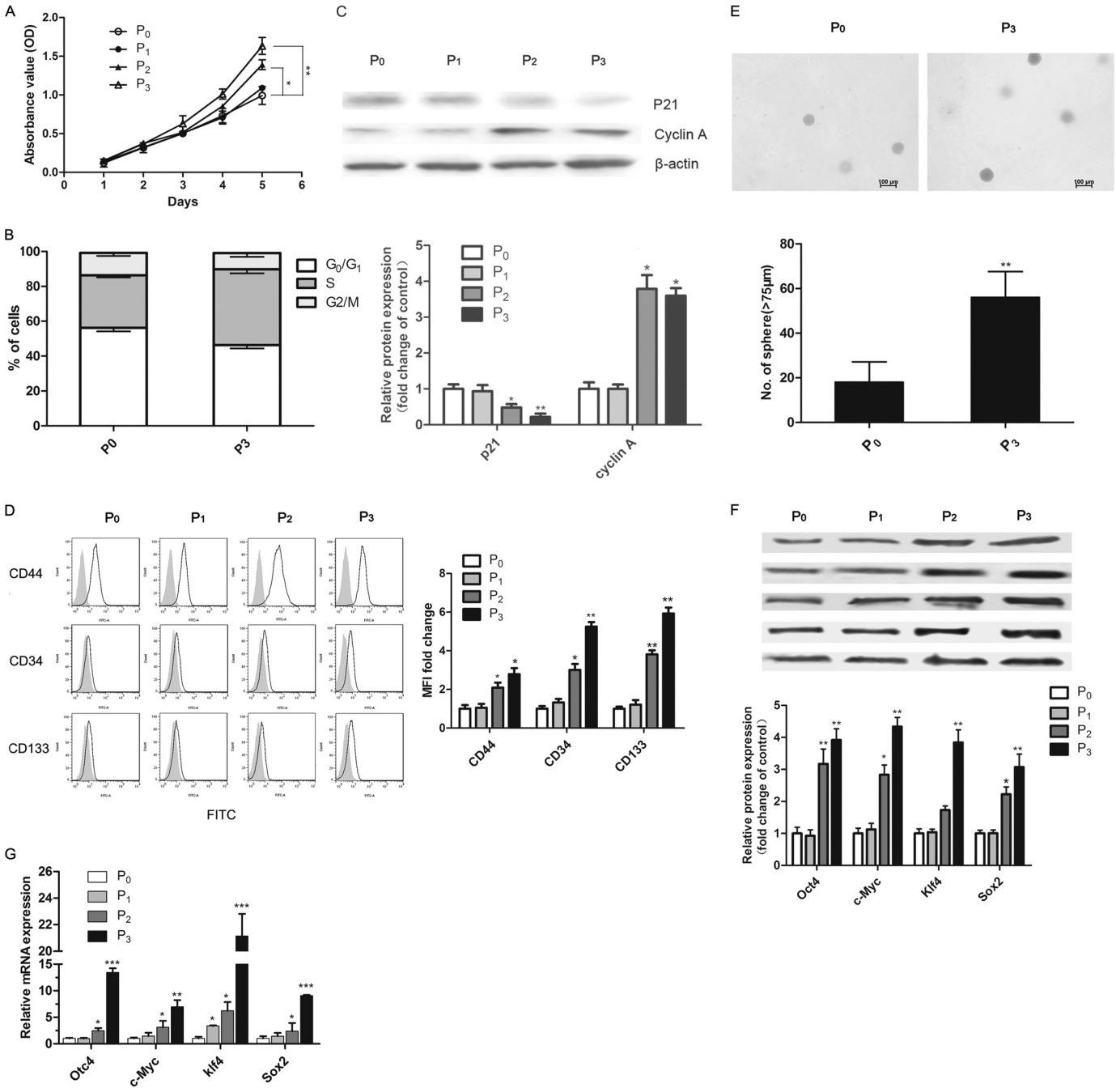

FIGURE 2. **The proliferation and stem-cell-like phenotype of immune-selected cancer cells.** *A*, the cell proliferation of P_0-P_3 cells was measured by MTT assay. *B*, the cell-cycle distribution of P_0 and P_3 cells. *C*, Western blot analysis of cell-cycle proteins expression including cyclin A and p21 in cells of each generation. β-Actin was used as a loading control. The relative expression of each protein = (density of each band/density of the indicated β-actin band). Values are represented as -fold increases relative to P_0. *D*, flow cytometry analysis of stem cell markers including CD44, CD34, and CD133 for Lewis lung cancer in the P_0–P_3 population. Representative histograms are shown in *D*, *left*. The *gray solid histogram* represents isotype control. Results of quantitative analysis are shown in *D*, *right*. *E*, representative images of tumor spheres formation derived from P_0 and P_3 cells. The microscopic fields were photographed (*upper*), and the number of *spheres* ≥75 μm was counted (*lower*). *F*, expression of stemness factors in cancer cells undergone *in vitro* immune selection was analyzed by Western blot. *G*, the mRNA levels of stemness factors were measured by real-time PCR and normalized to levels of GADPH mRNA. Data mentioned above are represented as the mean ± S.D. ($n \geq 5$ per group). *, $p < 0.05$; **, $p < 0.01$; ***, $p < 0.001$, *versus* P_0 cells.

it to generate tumors, whereas ~40% of mice challenged with 2×10^3 P_3 cells generated tumors. All of the mice challenged with 2×10^4 P_3 cells generated tumors. Tumor formation can be seen in nearly 30% of the mice challenged with 2×10^4 P_0 cells. Tumors in P_3-challenged mice were nearly twice the size of those in P_0-challenged mice. These data indicate that there is substantial enhancement of tumorigenicity in P_3 relative to P_0 cells.

The Role of CD47/TSP-1/SIRP-α Axis and Its Relationship with Tumors and the Microenvironment—Flow cytometry was utilized to determine CD47 expression on tumor cells. Results showed that there was prominent surface expression of CD47 on P_0 cells, and the CD47-associated fluorescence had a significant increase (about four times) as the immune selection drove cells to becoming P_3 cells (Fig. 4*A*). Simultaneously, the results

of immunofluorescence staining showed that compared with P_0 cells, almost all of the P_3 cells exhibited enhanced surface fluorescence of CD47 (Fig. 4*B*).

TSP-1 expression in normal lung tissues and LLC tumors from C57BL/6 mice was assessed by immunohistochemistry. TSP-1 expression was high in normal lung tissue but almost

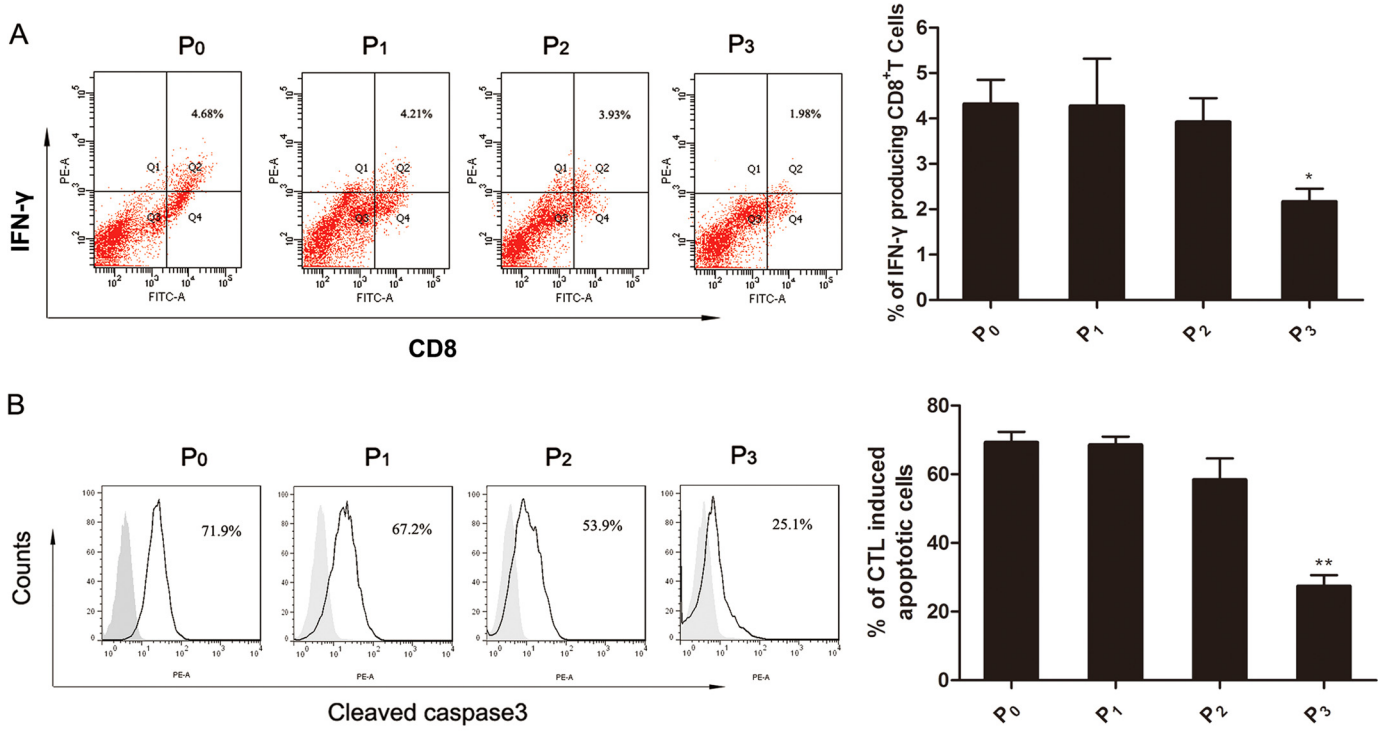

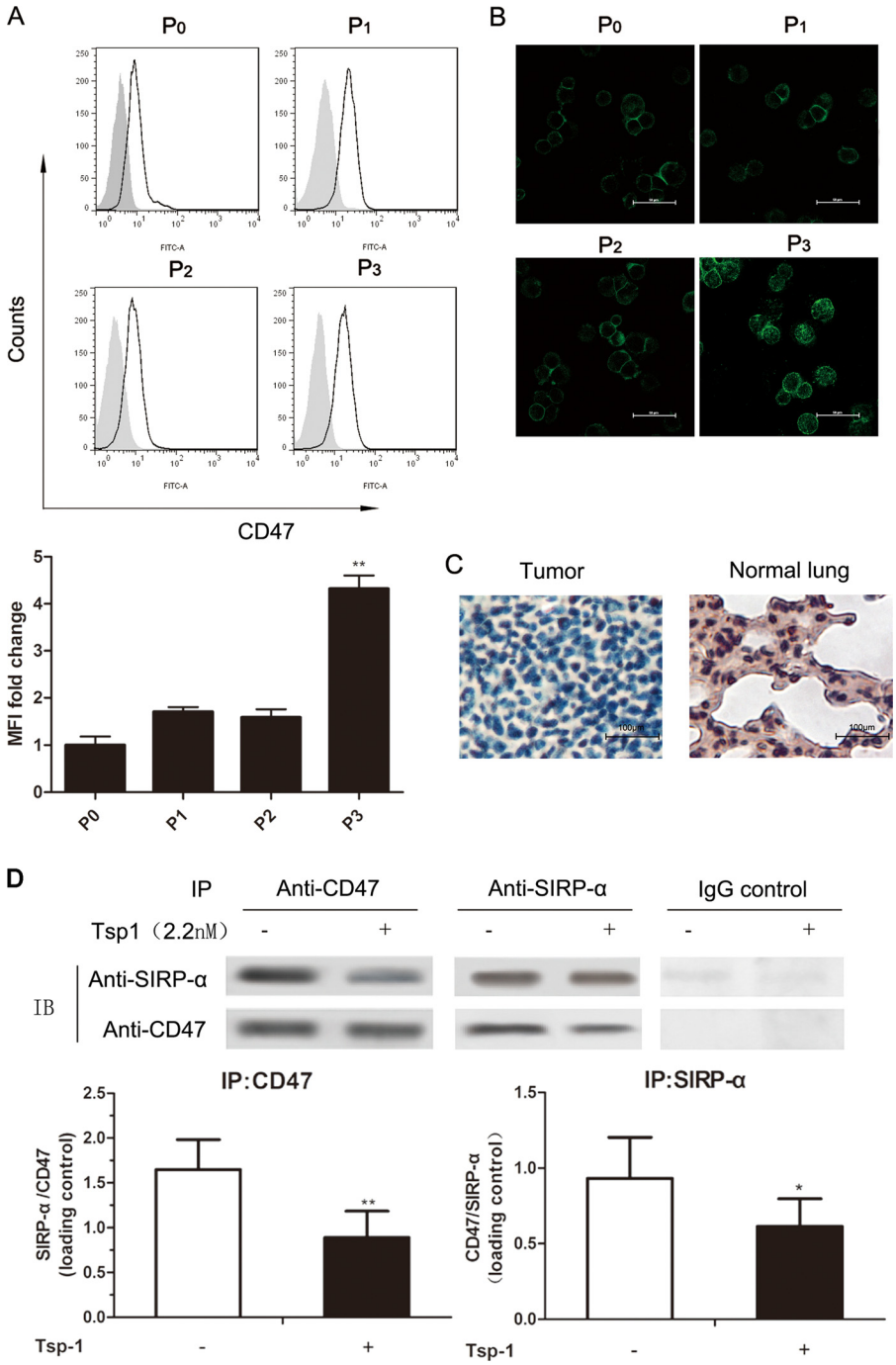

FIGURE 4. **The expression and the interaction of CD47 and its two ligands, TSP-1 and SIRP-α.** *A*, *upper*, representative histograms of the CD47 expression. The *gray solid histogram* represents isotype control. *A*, *lower*, the mean fluorescence intensity (*MFI*) of CD47 was normalized by that of isotype control. The expression of CD47 in cells of each generation is shown as -fold change in the mean fluorescence intensity compared with P_0. Data show a summary of a total of five independent experiments. *, $p < 0.05$; **, $p < 0.01$, *versus* P_0. *B*, representative confocal microscopy images of P_0–P_3 cells stained for CD47. *C*, representative images of TSP-1 expression by immunohistochemistry in normal mice lungs and lung adenocarcinomas. *D*, co-immunoprecipitation of CD47 with SIRP-α from co-culture lysates of immature DC cells and LLC cells with or without TSP-1 pretreatment. Representative blots (*IB*) are shown in the *upper graph*, whereas quantification of three independent Western blots is shown in the *lower graph*.

FIGURE 3. **The immunogenicity and tumorigenicity of immune-selected cells.** Spleen lymphocytes from vaccinated mice as effectors were fed with P_0-P_3 cells as targets. As effector cells, spleen lymphocytes were examined for the frequency of IFN-γ producing CD8+ T cells by flow cytometry. *A*, *left*, shows a summary, whereas *A*, *right*, shows representative dot plots. The frequency of apoptotic (cleaved-caspase-3 positive) tumor cells was measured by flow cytometry. Representative histograms of one of the experiments were shown in *B*, *left*). The *gray solid histogram* represents isotype control. *B*, *right*, shows quantitative analysis of the cleaved-caspase-3 expression. *C*, the cytotoxicity of CTL against P0-P3 cells was evaluated by a lactate dehydrogenase (*LDH*) release assay. *D*, the tumor formation of P_0 and P_3 cells *in vivo* was monitored for 18 days after tumor re-challenge at the indicated cell densities into nude mice. *E*, tumor weights were measured at the 18th day after re-challenge. Seven nude mice were included in each group. Values show a summary of >5 independent experiments. Data are represented as the mean ± S.D. *, $p < 0.05$; **, $p < 0.01$, compared with the P_0.

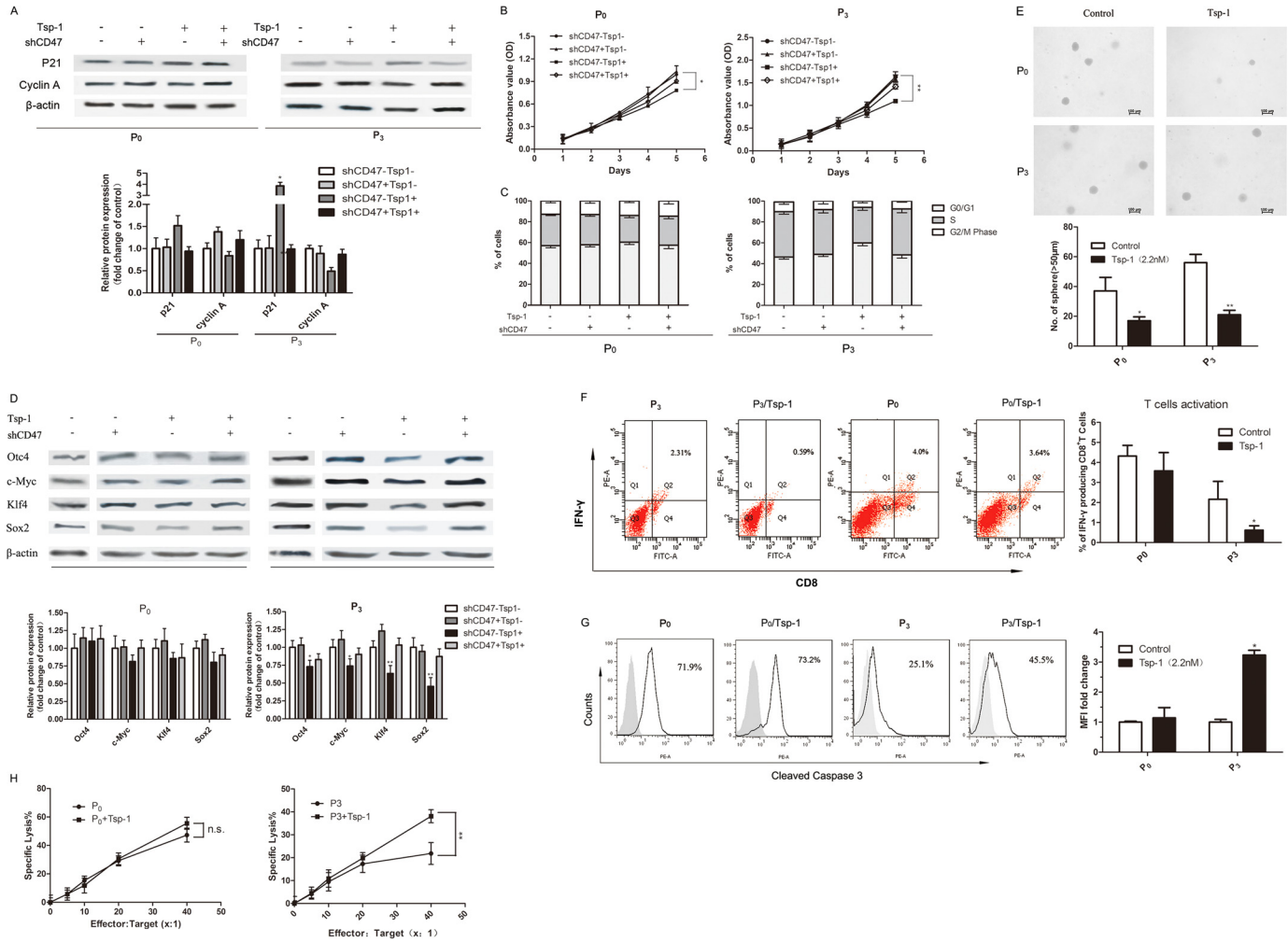

FIGURE 5. **TSP-1 prevented the stem-like and immune-resistant phenotype of immune-selected tumor cells in the presence of CD47.** *A*, Western blot analysis of the expression of cell-cycle proteins in P_0 and P_3 cells upon TSP-1/CD47 signal interference. *B*, cell proliferation of P_0-P_3 with or without TSP-1/CD47 signal interference. *C*, the impact of the TSP-1/CD47 signal on the cell-cycle distribution of P_0 and P_3 cells. *D*, the effect of the TSP-1/CD47 signal on the stemness factors expression in immune-selected cancer cells. β-Actin was used as a loading control. *E*, sphere-forming capacity of P_0 or P_3 cells treated with 2.2 nM TSP-1. *F*, P_0 and P_3 cells pretreated with 2.2 nM TSP-1 were incubated with CTLs for the indicated times. Representative dot plots (*left*) and a summary (*right*) of five experiments were shown. The population of IFN-γ-producing CD8+ T cells was measured by flow cytometry to detect CTL activation. *G*, P_0 and P_3 cells pretreated with 2.2 nM TSP-1 or not were co-incubated with tumor-specific CTLs, and the frequency of cleaved caspase-3+ cells was measured by flow cytometry. *H*, a lactate dehydrogenase release assay was also performed to evaluate the cytotoxicity of CTLs against P_0 and P_3 cells with TSP-1 treatment. Data above are the means of five independent experiments ± S.D. *, $p < 0.05$; **, $p < 0.01$, *versus* untreated; *ns*, not significant.

absent in lung adenocarcinomas (Fig. 4*C*) and immune-selected cell lines (data not shown).

LLC cells pretreated with 2.2 nM TSP-1 were co-cultured with immature DCs. The co-cultured cell lysates were then prepared and used for co-immunoprecipitation. Data in Fig. 4*D* showed that SIRP-α was co-precipitated with a CD47 monoclonal antibody. Conversely, CD47 was co-precipitated by a SIRP-α monoclonal antibody. An isotype-matched control IgG antibody did not co-precipitate either SIRP-α or TSP1. Importantly, we also found that TSP-1 pretreatment significantly inhibited co-immunoprecipitation between SIRP-α and CD47, whereas co-immunoprecipitation using tumor cell lysates that had not been co-cultured did not show similar results (data not shown).

These results suggest that TSP-1 is absent in normal LLC cells. Exogenous treatment of TSP-1 may be able to suppress the CD47-mediated tumor immune escape by disrupting the CD47-SIRP-a interaction. With the increasing surface expression of CD47, this suppression effect may be even more obvious in immune-selected cells.

Cooperation of TSP-1 and CD47 Undermined the Malignancy and Immunogenicity of Immune-selected Cells—To investigate whether the CD47/TSP-1 signal has an impact on tumor malignancy and immungenicity, we treated P_0 and P_3 cells with shCD47 vector or recombinant TSP-1. Then we characterized their growth rate, stem-like properties, and immune-resistant phenotype. The dose of TSP-1, the amount of transfected plasmid, and the incubation time were all optimized by preliminary experiments (data not shown).

Significantly, incubation of exogenous TSP-1 impaired cell proliferation in P_0 and P_3 cells. TSP-1 incubation also caused decreased cyclin A expression, increased p21 expression, and less cell distribution in S phase and G_2/M phase in P_3 cells (Fig. 5, *A*–*C*). It suggests changes in cell proliferation can be attributed to a perturbation of the cell cycle. P3 cells, which were pretreated with TSP-1, exhibited declined cancer stem-like

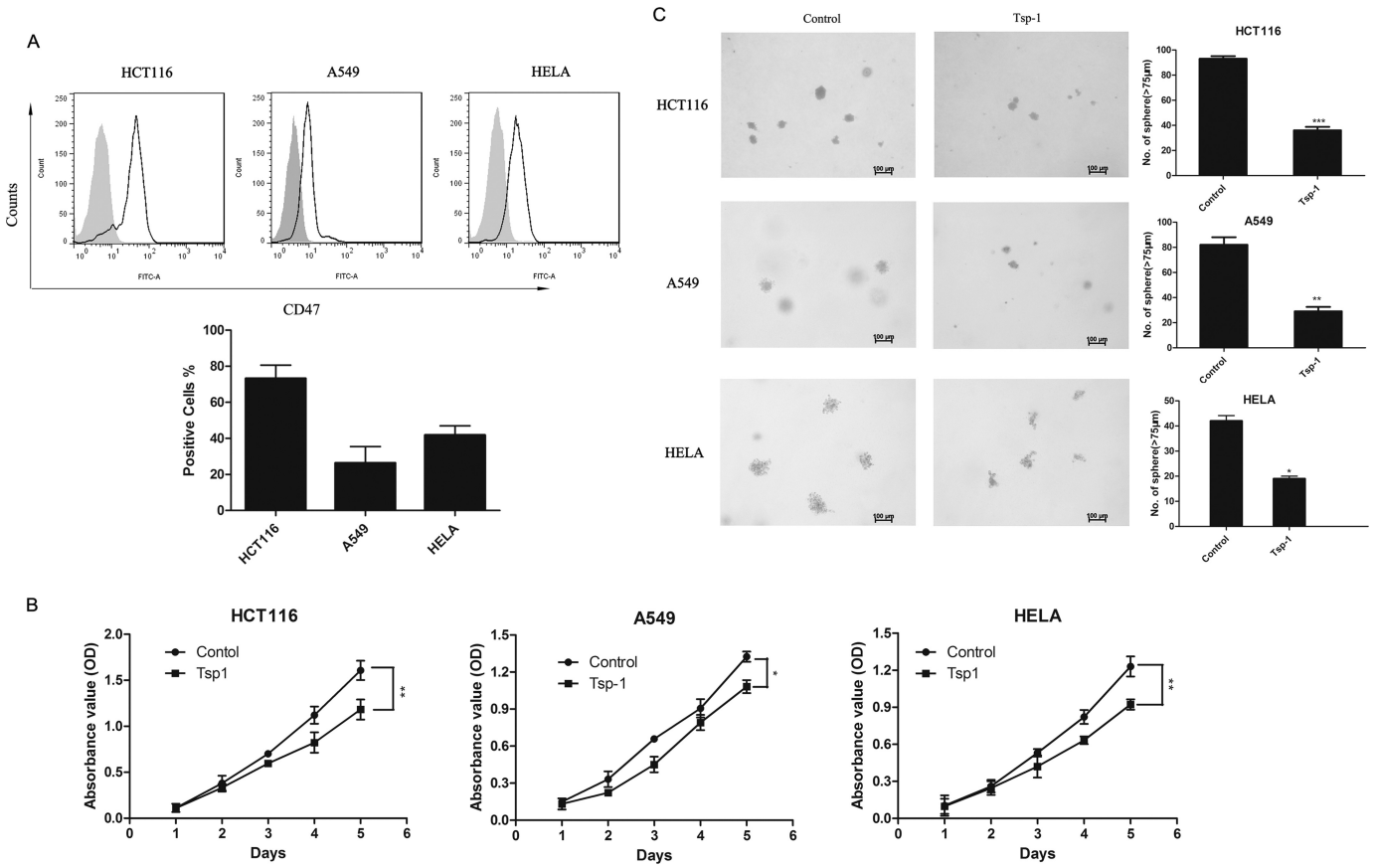

FIGURE 6. **TSP-1 also inhibited the cell proliferation and sphere-forming capacity of human cancer cells.** The expression of CD47 on the surface of A549, HCT116, and HeLa cells was measured by flow cytometry. *A*, *upper*, representative histograms show the expression of CD47. The *gray solid histogram* represents isotype control. *A*, *bottom*, the expression of CD47 is shown as the percentage of FITC-positive cells. *B*, the inhibitory effect of TSP-1 on the growth rate of human tumor cells including A549, HCT116, and HeLa. A549, HCT116, and HeLa cells were treated with 2.2 nM TSP-1 for indicated times. *C*, the sphere-forming capacity of these cells was analyzed in suspension culture. A summary of five independent experiments is shown. *, $p < 0.05$; **, $p < 0.01$; ***, $p < 0.001$.

properties including down-regulation of stemness factors (Fig. 5*D*) and poorer sphere-forming capacity (Fig. 5*E*). All of the results mentioned above could be reversed by CD47 knockdown. Interestingly, the same treatment had little effect on P_0 cells, probably due to the relatively low expression of cell surface CD47.

Next we explored the immune-resistant phenotype of P_0 or P_3 cells upon TSP-1 pretreatment. We first determined the frequency of IFN-γ-producing CD8+ cells. We found that pretreating tumor cells with TSP-1 resulted in remarkable suppression of IFN-γ-secreting CD8+ T cells (Fig. 5*F*). Furthermore, tumor cells that were pretreated with TSP-1 became more vulnerable to CTL (Fig. 5*G*). Consistent with the results obtained for caspase-3 activation and the lactate dehydrogenase assay, a larger degree of cytotoxicity was seen in TSP-1-pretreated P3 cells mixed with CTLs relative to untreated cells mixed with CTLs (Fig. 5*H*). Transfection of control shRNA vector had little effect on the results (data not shown).

Taken together, these results indicate that by co-operating with CD47, TSP-1 could override the malignancy, stem-like properties, and the immunogenicity brought by immune selection. These effects were much more prominent in P_3 cells than in P_0 cells, probably due to the up-regulation of CD47 in P_3.

The Therapeutic Effect of TSP-1 Is Also Effective across Different Human Cancer Lines—Having verified the role of the CD47/TSP-1 signal in mouse cancer cell line (LLC), we next profiled CD47 expression across a variety of human cancer cell lines including colon cancer (HCT116), non-small cell lung cancer (A549), and cervical cancer (HeLa). The results of flow cytometry showed that CD47 was present on the cell surface of all the human cancer lines we screened (Fig. 6*A*), which suggests TSP-1/CD47 regulation may be effective in these cells. We then assessed the effect of human recombinant TSP-1 on cell proliferation and tumor sphere formation. TSP-1 treatment slowed down the cell growth rate to different extents (Fig. 6*B*). Furthermore, cells pretreated with TSP-1 showed diminished sphere-forming capacity (Fig. 6*C*). These results demonstrate that TSP-1 is also therapeutically effective on some types of human cancer cell lines.

DISCUSSION

Previous studies have reported DC cells pulsed with PDT-treated tumor cells (PDT-DCs) can induce an anti-tumor immune response *in vivo* and, most importantly, is a potent vaccination strategy (6, 7, 40). Splenic lymphocytes isolated from vaccinated mice exhibited significant cytotoxicity against specific tumor cells (41, 42). According to the cancer immuno-

editing theory, in which heterogeneous tumors are attacked by host immune surveillance, most cancer cells will be eliminated in the early stage of vaccination. Rare cells may survive the elimination phase. Their immunogenicity and malignant properties can be sculpted. The cells that survive may then acquire the ability to circumvent immune recognition and/or destruction (13).

Based on this theory, in the present study we first established a system to select the tumor cells that succeed in escaping from the immune clearance of PDT-mediated vaccination. We termed this system "immune selection." Our data demonstrated that cells that had gone through immune selection exhibited enhanced proliferation and tumorigenicity. In addition, immune-selected cells also exhibited various hallmarks of cancer stem cells such as sphere-forming capacity and the exposure of stem cell markers as well as the expression of stemness factors. Although whether P_3 cells were definitively cancer stem cells was unclear, they showed more pronounced malignant features when compared with the parental cells (P_0). On this basis, we conclude that PDT-mediated vaccination has the ability to select for cancer stem cell-like phenotypes.

Furthermore, our data also showed that CD47 expression on the surface of immune-selected cells increased significantly. CD47 is pivotal in the TSP-1/CD47/SIRP-α signal axis, which serves as a bridge between tumors and the microenvironment. Therefore, we suspected that the interaction between CD47 and its two ligands, TSP-1 and SIRP-α, was responsible for the development of malignant and immunogenic properties.

Kaur *et al.* (43) have proven that in murine endothelial cells, loss of cell surface CD47 elevates the expression of stem cell transcription factors, which resulted in sustained cell proliferation, increased asymmetric division, and enhanced ability to form clusters. Based on this finding, CD47 expression appears to be a disadvantage for cells. For tumor cells, however, the results seem to be a paradox for the high expression of CD47. Our data also suggested that in LLC cells, knockdown of CD47 alone affected neither the expression of stemness factors nor the malignant phenotypes. Kaur *et al.* (43) attributed the phenomenon to the dysregulation of c-Myc. In our opinions, it is more likely to be due to the absence of TSP-1.

For the past 20 years TSP-1 has been recognized as an endogenous angiogenesis inhibitor (44–46). Little attention has been given to the effect of TSP-1 on tumor malignancy and immune response in a cell-extrinsic or -intrinsic manner. In fact, an increasing number of papers have reported the role of TSP-1 in these aspects (20, 47). As we have shown in the present study, TSP-1 treatment helped tumor cells restore the capacity of CD47 to inhibit the expression of stemness factors. In other words, the cooperation of CD47 and TSP-1 could negatively regulate the stemness factors. Further study is required to clarify if there is a negative feedback between CD47/TSP-1 and stemness factors and also to demonstrate the details of such a mechanism.

From the apparent efficacy, TSP-1 pretreatment can inhibit the malignant sculpture of the immune system on tumor cells. On the one hand, it could undermine a stem-like and highly tumorigenic phenotype in the P_3 cell line. On the other hand, TSP-1 could also enhance the cytotoxity of CTLs against P_3 cells, undermining the immune escape ability of immune-selected cells.

The ability of cells to escape immunosurveillance depends largely on the interaction among CD47, SIRP-α, and TSP-1. Burger *et al.* (17) observed that a conformational change in CD47 could switch the molecule from an anti-immunosurveillance signal into an activating one. When CD47 was bound by TSP-1, its conformation was altered, making SIRP-α fail to recognize CD47 normally (17). Isenberg *et al.* (48) confirmed that TSP-1 could bind to CD47 with a higher affinity than SIRP-α, so it was able to block the interaction between CD47 and SIRP-α . In light of these studies and our own research, we postulated that treatment of tumor cells with TSP-1 competitively blocked the interaction between SIRP-α and CD47 by fixing the conformation of CD47, thus interfering with the documented mechanism of immune escape mediated by the CD47/SIRP-α signal (19). Further research will be necessary to give more insights into this interaction.

The hypotheses mentioned above can in turn partly explain the evolutionary process of tumor cells in response to CTL-mediated killing. For the intrinsic absence of TSP-1 in tumor cells, the inhibitory effect on stemness factors, which depends on the cooperation of CD47 and TSP-1, did not work. Therefore, despite the increasing cell-surface exposure of CD47, stemness factors including c-Myc, Oct4, Klf4, and Sox2 were up-regulated significantly upon the stimulus of CTL killing. The overexpression of stemness factors was previously reported to be capable of conferring tumor cell-enhanced malignant properties such as proliferation or survival. In addition, the formation of stem-like phenotype may also be attributed to the up-regulation of these stemness factors (49–52). Meanwhile, the absence of TSP-1 promoted the interaction of CD47 and SIRP-α, which interferes with the cross-talk between DC cells and tumor cells and weakens the activation of CTL. As a result, tumor cells exhibited immune-resistant phenotype on the whole.

Of note, even though almost all the P_3 cells exhibited enhanced CD47-associated fluorescence, we cannot conclude that immune selection induces the cells to express more CD47. It is also possible that immune selection selects a subpopulation with high levels of CD47, which enable immune-selected tumor cells to show enhanced malignant characteristics and the ability for immune escape. Additional studies are needed to clarify these points.

In our experiments recombinant mouse TSP-1 protein was used to act directly on the tumor cells. However, the same experimental method is very difficult to implement *in vivo*. Direct injection of TSP-1 in any manner may also have an impact on the other cells in the tumor microenvironment, which may make the results quite different from the data *in vitro*. Therefore, for successful *in vivo* experiments, we plan to conduct stable cell lines that overexpress the TSP-1 protein, thus investigating if the results are consistent with those in the present study. By conducting a stable cell line, we will also continue to explore the interference effects of TSP-1 *in vivo*.

In summary, our study showed there was an emergence of a stem-like and immune-resistant phenotype in tumor cells in response to PDT-mediated tumor vaccination. Furthermore,

our data demonstrate for the first time that the function shift of the TSP-1/CD47/SIRP-α signal axis has a prominent impact on the malignant phenotype and the immune escape of tumor cells. Treatment of tumor cells with TSP-1 in the presence of CD47 was proven to be an effective strategy to overcome malignant transformation. Our findings raise new challenges for immunotherapy and also provide a research foundation to overcome the problem.

REFERENCES

1. Sharma, P., Wagner, K., Wolchok, J. D., and Allison, J. P. (2011) Novel cancer immunotherapy agents with survival benefit: recent successes and next steps. *Nat. Rev. Cancer* **11,** 805–812
2. Liu, T., Wu, L. Y., Choi, J. K., and Berkman, C. E. (2010) Targeted photodynamic therapy for prostate cancer: inducing apoptosis via activation of the caspase-8/-3 cascade pathway. *Int. J. Oncol.* **36,** 777–784
3. Galluzzi, L., Kepp, O., and Kroemer, G. (2012) Enlightening the impact of immunogenic cell death in photodynamic cancer therapy. *EMBO J.* **31,** 1055–1057
4. Garg, A. D., Nowis, D., Golab, J., and Agostinis, P. (2010) Photodynamic therapy: illuminating the road from cell death towards anti-tumour immunity. *Apoptosis* **15,** 1050–1071
5. Garg, A. D., Krysko, D. V., Vandenabeele, P., and Agostinis, P. (2012) Hypericin-based photodynamic therapy induces surface exposure of damage-associated molecular patterns like HSP70 and calreticulin. *Cancer Immunol. Immunother.* **61,** 215–221
6. Garg, A. D., Krysko, D. V., Verfaillie, T., Kaczmarek, A., Ferreira, G. B., Marysael, T., Rubio, N., Firczuk, M., Mathieu, C., Roebroek, A. J., Annaert, W., Golab, J., de Witte, P., Vandenabeele, P., and Agostinis, P. (2012) A novel pathway combining calreticulin exposure and ATP secretion in immunogenic cancer cell death. *EMBO J.* **31,** 1062–1079
7. Jung, N. C., Kim, H. J., Kang, M. S., Lee, J. H., Song, J. Y., Seo, H. G., Bae, Y. S., and Lim, D. S. (2012) Photodynamic therapy-mediated DC immunotherapy is highly effective for the inhibition of established solid tumors. *Cancer Lett.* **324,** 58–65
8. Palucka, K., and Banchereau, J. (2012) Cancer immunotherapy via dendritic cells. *Nat. Rev. Cancer* **12,** 265–277
9. Schatton, T., and Frank, M. H. (2009) Antitumor immunity and cancer stem cells. *Ann. N.Y. Acad. Sci.* **1176,** 154–169
10. Aptsiauri, N., Carretero, R., Garcia-Lora, A., Real, L. M., Cabrera, T., and Garrido, F. (2008) Regressing and progressing metastatic lesions: resistance to immunotherapy is predetermined by irreversible HLA class I antigen alterations. *Cancer Immunol. Immunother.* **57,** 1727–1733
11. Wilczyński, J. R., and Duechler, M. (2010) How do tumors actively escape from host immunosurveillance? *Arch. Immunol. Ther. Exp. (Warsz)* **58,** 435–448
12. Noh, K. H., Lee, Y. H., Jeon, J. H., Kang, T. H., Mao, C. P., Wu, T. C., and Kim, T. W. (2012) Cancer vaccination drives Nanog-dependent evolution of tumor cells toward an immune-resistant and stem-like phenotype. *Cancer Res.* **72,** 1717–1727
13. Schreiber, R. D., Old, L. J., and Smyth, M. J. (2011) Cancer immunoediting: integrating immunity's roles in cancer suppression and promotion. *Science* **331,** 1565–1570
14. Brown, E. J., and Frazier, W. A. (2001) Integrin-associated protein (CD47) and its ligands. *Trends Cell Biol.* **11,** 130–135
15. Sarfati, M., Fortin, G., Raymond, M., and Susin, S. (2008) CD47 in the immune response: role of thrombospondin and SIRP-α reverse signaling. *Curr. Drug Targets* **9,** 842–850
16. Willingham, S. B., Volkmer, J. P., Gentles, A. J., Sahoo, D., Dalerba, P., Mitra, S. S., Wang, J., Contreras-Trujillo, H., Martin, R., Cohen, J. D., Lovelace, P., Scheeren, F. A., Chao, M. P., Weiskopf, K., Tang, C., Volkmer, A. K., Naik, T. J., Storm, T. A., Mosley, A. R., Edris, B., Schmid, S. M., Sun, C. K., Chua, M. S., Murillo, O., Rajendran, P., Cha, A. C., Chin, R. K., Kim, D., Adorno, M., Raveh, T., Tseng, D., Jaiswal, S., Enger, P. Ø., Steinberg, G. K., Li, G., So, S. K., Majeti, R., Harsh, G. R., van de Rijn, M., Teng, N. N., Sunwoo, J. B., Alizadeh, A. A., Clarke, M. F., and Weissman, I. L. (2012) The CD47-signal regulatory protein α (SIRPa) interaction is a therapeutic target for human solid tumors. *Proc. Natl. Acad. Sci. U.S.A.* **109,** 6662–6667
17. Burger, P., Hilarius-Stokman, P., de Korte, D., van den Berg, T. K., and van Bruggen, R. (2012) CD47 functions as a molecular switch for erythrocyte phagocytosis. *Blood* **119,** 5512–5521
18. Zhao, X. W., van Beek, E. M., Schornagel, K., Van der Maaden, H., Van Houdt, M., Otten, M. A., Finetti, P., Van Egmond, M., Matozaki, T., Kraal, G., Birnbaum, D., van Elsas, A., Kuijpers, T. W., Bertucci, F., and van den Berg, T. K. (2011) CD47-signal regulatory protein-α (SIRPα) interactions form a barrier for antibody-mediated tumor cell destruction. *Proc. Natl. Acad. Sci. U.S.A.* **108,** 18342–18347
19. Chao, M. P., Weissman, I. L., and Majeti, R. (2012) The CD47-SIRPα pathway in cancer immune evasion and potential therapeutic implications. *Curr. Opin. Immunol.* **24,** 225–232
20. Miller, T. W., Kaur, S., Ivins-O'Keefe, K., and Roberts, D. D. (2013) Thrombospondin-1 is a CD47-dependent endogenous inhibitor of hydrogen sulfide signaling in T cell activation. *Matrix Biol.* **32,** 316–324
21. Grimbert, P., Bouguermouh, S., Baba, N., Nakajima, T., Allakhverdi, Z., Braun, D., Saito, H., Rubio, M., Delespesse, G., and Sarfati, M. (2006) Thrombospondin/CD47 interaction: a pathway to generate regulatory T cells from human CD4+ CD25- T cells in response to inflammation. *J. Immunol.* **177,** 3534–3541
22. Kaur, S., Martin-Manso, G., Pendrak, M. L., Garfield, S. H., Isenberg, J. S., and Roberts, D. D. (2010) Thrombospondin-1 inhibits VEGF receptor-2 signaling by disrupting its association with CD47. *J. Biol. Chem.* **285,** 38923–38932
23. Dasgupta, P., Rizwani, W., Pillai, S., Davis, R., Banerjee, S., Hug, K., Lloyd, M., Coppola, D., Haura, E., and Chellappan, S. P. (2011) ARRB1-mediated regulation of E2F target genes in nicotine-induced growth of lung tumors. *J. Natl. Cancer Inst.* **103,** 317–333
24. Vermeer, D. W., Spanos, W. C., Vermeer, P. D., Bruns, A. M., Lee, K. M., and Lee, J. H. (2013) Radiation-induced loss of cell surface CD47 enhances immune-mediated clearance of human papillomavirus-positive cancer. *Int. J. Cancer* **133,** 120–129
25. Ma, L., Mao, R., Shen, K., Zheng, Y., Li, Y., Liu, J., and Ni, L. (2014) Atractylenolide I-mediated Notch pathway inhibition attenuates gastric cancer stem cell traits. *Biochem. Biophys. Res. Commun.* **450,** 353–359
26. Zheng, Y., Le, V., Cheng, Z., Xie, S., Li, H., Tian, J., and Liu, J. (2013) Development of rapid and highly sensitive HSPA1A promoter-driven luciferase reporter system for assessing oxidative stress associated with low-dose photodynamic therapy. *Cell Stress Chaperones* **18,** 203–213
27. Ramakrishnan, R., Assudani, D., Nagaraj, S., Hunter, T., Cho, H. I., Antonia, S., Altiok, S., Celis, E., and Gabrilovich, D. I. (2010) Chemotherapy enhances tumor cell susceptibility to CTL-mediated killing during cancer immunotherapy in mice. *J. Clin. Invest.* **120,** 1111–1124
28. Shirota, Y., Shirota, H., and Klinman, D. M. (2012) Intratumoral injection of CpG oligonucleotides induces the differentiation and reduces the immunosuppressive activity of myeloid-derived suppressor cells. *J. Immunol.* **188,** 1592–1599
29. Di Stefano, B., Prigione, A., and Broccoli, V. (2009) Efficient genetic reprogramming of unmodified somatic neural progenitors uncovers the essential requirement of Oct4 and Klf4. *Stem Cells Dev.* **18,** 707–716
30. Livak, K. J., and Schmittgen, T. D. (2001) Analysis of relative gene expression data using real-time quantitative PCR and the $2(-\Delta\Delta C(T))$ method. *Methods* **25,** 402–408
31. Shen, K., Liang, Q., Xu, K., Cui, D., Jiang, L., Yin, P., Lu, Y., Li, Q., and Liu, J. (2012) MiR-139 inhibits invasion and metastasis of colorectal cancer by targeting the type I insulin-like growth factor receptor. *Biochem. Pharmacol.* **84,** 320–330
32. Morrison, B. J., Steel, J. C., and Morris, J. C. (2012) Sphere culture of murine lung cancer cell lines are enriched with cancer initiating cells. *PloS ONE* **7,** e49752
33. Fucikova, J., Kralikova, P., Fialova, A., Brtnicky, T., Rob, L., Bartunkova, J., and Spísek, R. (2011) Human tumor cells killed by anthracyclines induce a tumor-specific immune response. *Cancer Res.* **71,** 4821–4833
34. Mroz, P., Szokalska, A., Wu, M. X., and Hamblin, M. R. (2010) Photodynamic therapy of tumors can lead to development of systemic antigen-

specific immune response. *PloS ONE* **5,** e15194
35. Rivera, C., Rivera, S., Loriot, Y., Vozenin, M. C., and Deutsch, E. (2011) Lung cancer stem cell: new insights on experimental models and preclinical data. *J. Oncol.* **2011,** 549181
36. Huang, C. P., Tsai, M. F., Chang, T. H., Tang, W. C., Chen, S. Y., Lai, H. H., Lin, T. Y., Yang, J. C., Yang, P. C., Shih, J. Y., and Lin, S. B. (2013) ALDH-positive lung cancer stem cells confer resistance to epidermal growth factor receptor tyrosine kinase inhibitors. *Cancer Lett.* **328,** 144–151
37. Zhang, A. M., Fan, Y., Yao, Q., Ma, H., Lin, S., Zhu, C. H., Wang, X. X., Liu, J., Zhu, B., Sun, J. G., and Chen, Z. T. (2012) Identification of a cancer stem-like population in the Lewis lung cancer cell line. *Asian Pac. J. Cancer Prev.* **13,** 761–766
38. Eramo, A., Lotti, F., Sette, G., Pilozzi, E., Biffoni, M., Di Virgilio, A., Conticello, C., Ruco, L., Peschle, C., and De Maria, R. (2008) Identification and expansion of the tumorigenic lung cancer stem cell population. *Cell Death Differ.* **15,** 504–514
39. Tirino, V., Camerlingo, R., Franco, R., Malanga, D., La Rocca, A., Viglietto, G., Rocco, G., and Pirozzi, G. (2009) The role of CD133 in the identification and characterisation of tumour-initiating cells in non-small-cell lung cancer. *Eur. J. Cardiothorac. Surg.* **36,** 446–453
40. Korbelik, M., and Merchant, S. (2012) Photodynamic therapy-generated cancer vaccine elicits acute phase and hormonal response in treated mice. *Cancer Immunol. Immunother.* **61,** 1387–1394
41. Kabingu, E., Vaughan, L., Owczarczak, B., Ramsey, K. D., and Gollnick, S. O. (2007) CD8+ T cell-mediated control of distant tumours following local photodynamic therapy is independent of CD4+ T cells and dependent on natural killer cells. *Br. J. Cancer* **96,** 1839–1848
42. Agostinis, P., Berg, K., Cengel, K. A., Foster, T. H., Girotti, A. W., Gollnick, S. O., Hahn, S. M., Hamblin, M. R., Juzeniene, A., Kessel, D., Korbelik, M., Moan, J., Mroz, P., Nowis, D., Piette, J., Wilson, B. C., and Golab, J. (2011) Photodynamic therapy of cancer: an update. *CA Cancer J. Clin.* **61,** 250–281
43. Kaur, S., Soto-Pantoja, D. R., Stein, E. V., Liu, C., Elkahloun, A. G., Pendrak, M. L., Nicolae, A., Singh, S. P., Nie, Z., Levens, D., Isenberg, J. S., and Roberts, D. D. (2013) Thrombospondin-1 signaling through CD47 inhibits self-renewal by regulating c-Myc and other stem cell transcription factors. *Sci. Rep.* **3,** 1673
44. Lawler, J. (2002) Thrombospondin-1 as an endogenous inhibitor of angiogenesis and tumor growth. *J. Cell. Mol. Med.* **6,** 1–12
45. Bornstein, P. (2009) Thrombospondins function as regulators of angiogenesis. *J. Cell Commun. Signal.* **3,** 189–200
46. Taraboletti, G., Rusnati, M., Ragona, L., and Colombo, G. (2010) Targeting tumor angiogenesis with TSP-1-based compounds: rational design of antiangiogenic mimetics of endogenous inhibitors. *Oncotarget* **1,** 662–673
47. Baek, K. H., Bhang, D., Zaslavsky, A., Wang, L. C., Vachani, A., Kim, C. F., Albelda, S. M., Evan, G. I., and Ryeom, S. (2013) Thrombospondin-1 mediates oncogenic Ras-induced senescence in premalignant lung tumors. *J. Clin. Invest.* **123,** 4375–4389
48. Isenberg, J. S., Annis, D. S., Pendrak, M. L., Ptaszynska, M., Frazier, W. A., Mosher, D. F., and Roberts, D. D. (2009) Differential interactions of thrombospondin-1, -2, and -4 with CD47 and effects on cGMP signaling and ischemic injury responses. *J. Biol. Chem.* **284,** 1116–1125
49. Liu, W., Le, A., Hancock, C., Lane, A. N., Dang, C. V., Fan, T. W., and Phang, J. M. (2012) Reprogramming of proline and glutamine metabolism contributes to the proliferative and metabolic responses regulated by oncogenic transcription factor c-MYC. *Proc. Natl. Acad. Sci. U.S.A.* **109,** 8983–8988
50. Chiou, S. H., Wang, M. L., Chou, Y. T., Chen, C. J., Hong, C. F., Hsieh, W. J., Chang, H. T., Chen, Y. S., Lin, T. W., Hsu, H. S., and Wu, C. W. (2010) Coexpression of Oct4 and Nanog enhances malignancy in lung adenocarcinoma by inducing cancer stem cell-like properties and epithelial-mesenchymal transdifferentiation. *Cancer Res.* **70,** 10433–10444
51. Herreros-Villanueva, M., Zhang, J. S., Koenig, A., Abel, E. V., Smyrk, T. C., Bamlet, W. R., de Narvajas, A. A., Gomez, T. S., Simeone, D. M., Bujanda, L., and Billadeau, D. D. (2013) SOX2 promotes dedifferentiation and imparts stem cell-like features to pancreatic cancer cells. *Oncogenesis* **2,** e61
52. Wang, W. J., Wu, S. P., Liu, J. B., Shi, Y. S., Huang, X., Zhang, Q. B., and Yao, K. T. (2013) MYC regulation of CHK1 and CHK2 promotes radioresistance in a stem cell-like population of nasopharyngeal carcinoma cells. *Cancer Res.* **73,** 1219–1231